Neuro-Oncology 15(7):880–890, 2013.
doi:10.1093/neuonc/not030
Advance Access publication March 21, 2013

In vitro and in vivo radiosensitization induced by hydroxyapatite nanoparticles

Sheng-Hua Chu, Surya Karri, Yan-Bin Ma, Dong-Fu Feng, and Zhi-Qiang Li

Department of Neurosurgery, Shanghai 3rd People's Hospital, School of Medicine, Shanghai Jiao Tong University, Shanghai, China (S.-H.C., Y.-B.M., D.-F.F.); Wellman Center for Photomedicine, Massachusetts General Hospital, Harvard Medical School, Boston, Massachusetts (S.-H.C.); Department of Neurosurgery, Massachusetts General Hospital, Harvard Medical School, Boston, Massachusetts (S.K.); Department of Neurosurgery, Zhongnan Hospital of Wuhan University, Wuhan, China (Z.-Q.L.)

Background. Previous study showed that hydroxyapatite nanoparticles (nano-HAPs) inhibited glioma growth in vitro and in vivo; and in a drug combination, they could reduce adverse reactions. We investigated the possible enhancement of radiosensitivity induced by nano-HAPs.

Methods. In vitro radiosensitization of nano-HAPs was measured using a clonogenic survival assay in human glioblastoma U251 and breast tumor brain metastatic tumor MDA-MB-231BR cells. DNA damage and repair were measured using γH2AX foci, and mitotic catastrophe was determined by immunostaining. The effect of nano-HAPs on in vivo tumor radiosensitivity was investigated in a subcutaneous and an orthotopic model.

Results. Nano-HAPs enhanced each cell line's radiosensitivity when the exposure was 1 h before irradiation, and they had no significant effect on irradiation-induced apoptosis or on the activation of the G_2 cell cycle checkpoint. The number of γH2AX foci per cell was significantly large at 24 h after the combination modality of nano-HAPs + irradiation compared with single treatments. Mitotic catastrophe was also significantly increased at an interval of 72 h in tumor cells receiving the combined modality compared with the individual treatments. In a subcutaneous model, nano-HAPs caused a larger than additive increase in tumor growth delay. In an orthotopic model, nano-HAPs significantly reduced tumor growth and extended the prolongation of survival induced by irradiation.

Conclusions. These results show that nano-HAPs can enhance the radiosensitivity of tumor cells in vitro and in vivo through the inhibition of DNA repair, resulting in an increase in mitotic catastrophe.

Keywords: rain metastatic tumor, glioblastoma, hydroxyapatite nanoparticles, irradiation, radiosensitization.

Malignant brain tumors found commonly occurring in adults, such as glioblastoma multiforme (GBM) and brain metastatic tumors, are characterized by their dissemination and invasiveness, inducing frequent recurrence of those tumors even after surgery and/or chemotherapy and radiotherapy.[1,2] Temozolomide given concurrently with radiotherapy significantly increases overall survival of GBM patients from 12.1 to 14.6 months compared with radiotherapy alone[3]; however, the survival rate remains low, prompting researchers to seek alternate treatments through better understanding of cell biology and novel therapeutic strategies that may supplement current treatments.[4]

With the development of nanotechnology, a new inorganic material, hydroxyapatite nanoparticles (nano-HAPs), was found to be able to inhibit the proliferation of tumor cells.[5,6] Our previous study[7] showed that not only could nano-HAPs inhibit the growth of glioma cells in vitro and in vivo, but they could also reduce poisonous, adverse reactions to BCNU (biscloroethylnitrosourea, carmustine), strongly cooperate with and decrease the toxicity of certain other chemotherapy drugs, and might also become a new clinical antineoplastic drug class. In the current study, we sought to investigate the effect of nano-HAPs on the radiosensitization of human glioblastoma U251 and human breast tumor brain metastatic tumor MDA-MB-231BR cells and their mechanism, to provide a theoretical basis for clinical use. The data presented show that nano-HAPs enhance the radiosensitivity of tumor cells in vitro and in vivo. In addition, this sensitization relates to delayed

Received August 21, 2012; accepted February 8, 2013.

Corresponding Author: Dr Sheng-Hua Chu, PhD, Department of Neurosurgery, Shanghai 3rd People's Hospital, School of Medicine, Shanghai Jiao Tong University, Shanghai 201900, China (shenghuachu@126.com).

dispersion of γH2AX foci, suggesting an inhibition of DNA repair.

Materials and Methods

Cell Lines and Treatment

Human GBM U251 (Wuhan University) and breast tumor brain metastatic tumor MDA-MB-231BR cells (American Type Culture Collection) were cultured in RPMI-1640 (Roswell Park Memorial Institute medium; Gibco Life Technologies) supplemented with 10% fetal bovine serum and penicillin-streptomycin. Nano-HAPs, provided by the East China University of Science and Technology Institute of Biomaterials, was dissolved in dimethyl sulfoxide to a concentration of 10 mg/L and stored at −80°C. For in vivo administration, nano-HAPs were suspended in saline solution. Cultures were irradiated using a Pantak X-ray source at a dose rate of 2 Gy/min.

Clonogenic Survival Assay

Clonogenic assay was done as previously described.[8,9] A specified number of cells were seeded into each well of a 6-well tissue culture plate. The cultures got the vehicle control dimethyl sulfoxide or nano-HAPs for 1 h before irradiation after allowing cells time to attach for 6 h; medium was removed and then replaced with medium free of nano-HAPs. Colonies were stained with crystal violet 12 days after seeding, and thereafter the number of colonies containing at least 50 cells and surviving fractions were calculated. Survival curves were then made after normalizing for the cytotoxicity induced by nano-HAPs alone. Each assay was performed in triplicate.

Flow Cytometry Analysis of Cell Cycle

The phase distribution of the cell cycle was evaluated using flow cytometry. The protocols of treatment were the same as in the clonogenic assay, except that the tumor cells were seeded into 10-cm dishes. Cultures were collected for fixation, then stained with propidium iodide, and phases were determined using flow cytometry. To evaluate the G_2 cell cycle checkpoint activation, mitotic cells were distinguished from G_2 cells, and the mitotic index was evaluated according to γH2AX expression detected in the tetraploid (4N) DNA content population as previously described.[9] In this assay, decreased mitotic index reflected onset of G_2 arrest. Each assay was performed in triplicate.

Apoptosis Assay

Apoptosis was quantitated using the Guava Nexin assay following the manufacturer's instructions. Samples with 2000 cells per well were gained on a Guava EasyCyte flow cytometer.

γH2AX Assay

Cells cultured in chamber slides were washed once with phosphate buffered saline (PBS) and then fixed in 4% formaldehyde in PBS for 10 min at room temperature. Cells were permeabilized and blocked with blocking buffer (5% normal goat serum, 0.2% Triton X-100 in PBS) for 1 h and incubated with anti-γH2AX monoclonal antibody (1:100; Upstate Biotechnology) overnight at 4°C. After washing twice with PBS, cells were incubated with fluorescein isothiocyanate–labeled rabbit anti-mouse antibody (1:100) for 1 h and washed twice with PBS. Nuclei were counterstained with 4′,6-diamidino-2-phenylindole (DAPI; 1 μg/mL) in PBS for 30 min before cells were covered by anti-fade solution (Fisher) and mounted. Slides were examined on a Leica Digital Module R XA fluorescent microscope. Images were captured by a Photometrics Sensys charge-coupled device camera (Roper Scientific) and imported into an IP Labs image analysis software package (Scanalytics). For each treatment condition, γH2AX foci were determined in at least 50 cells. Each assay was performed in triplicate.

Mitotic Catastrophe

The presence of fragmented nuclei was used to define cells undergoing mitotic catastrophe, as previously described.[9,10] Cells were fixed with methanol for 15 min at −20°C and stained overnight at 4°C with rabbit anti–α-tubulin antibody (Sigma) followed by staining with Texas Red–conjugated secondary antibody (Jackson ImmunoResearch) for 2 h at room temperature. Nuclei were counterstained with DAPI (Sigma). A single field containing 300 cells was chosen randomly for each treatment and photographed with epifluorescence. The presence of 2 or more distinct nuclear lobes within a single cell defined the nuclear fragmentation. Each assay was performed in triplicate.

Tumor Growth Delay Assay

Four to six-week-old BALB/c athymic nude male mice were subcutaneously injected with 5×10^6 tumor cells into the lateral aspect of the right leg. Tumors were irradiated locally using a Pantak irradiator with nude mice restrained in a custom lead jig. When tumors reached 172 mm^3 (7 × 7 mm), the nude mice were randomized into 4 groups: vehicle alone, nano-HAPs alone, irradiation (4 Gy) alone, and nano-HAPs + irradiation. The nude mice were given a single dose of nano-HAPs (10 mg/kg) by injection through the tail vein 1 h before local tumor irradiation (4 Gy). Tumor diameters were measured every 2 days with digital calipers, and the tumor volume, in cubic millimeters, was calculated by the formula: $\text{volume} = (\text{width})^2 \times \text{length}/2$.[7,11] Tumors were measured until the mean group tumor volume was >2000 mm^3. Each experimental group contained 10 nude mice. The animal experiments in this study were performed in compliance with the guidelines

of the Shanghai Jiao Tong University School of Medicine and Wuhan University.

Tumor Growth and Animal Survival in the Orthotopic Nude Mice Model

Eight-week-old BALB/c athymic nude male mice were anesthetized and stereotactically inoculated with tumor cells (10^4 cells in 2 μL PBS) into the left forebrain (1 mm anterior, 2 mm lateral to bregma, at 3 mm depth from skull surface). The animal experiments in this study were performed in compliance with the guidelines of the Medical School Institutes at Shanghai Jiao Tong University and Wuhan University. Animals were randomized into 4 treatment groups: control, nano-HAPs, irradiation, and nano-HAPs + irradiation ($n = 10$ each). Nano-HAPs treatment (10 mg/kg twice daily) started on day 1 after tumor inoculation and was administered 5 days weekly until the end of observation. Irradiation was delivered on day 4 to the entire head of each anesthetized nude mouse (6 Gy single dose) using a 6-megavolt linear accelerator. On day 15, tumor imaging in animal models was performed with a small animal coil on a high-field GE Signa 3T clinical MR scanner, and images were obtained using a standard T1 protocol following intraperitoneal injection of gadolinium diethylenetriamine pentaacetic acid (100 μL/20 g; Magnevist, Berlex Laboratories) 10 min before examination. The scanning parameters were axial T1 fast spin echo series-scan plane in enhanced scanning: phase field of view: 0.60; oblique field of view: 5.0; spacing: 0.0 mm; slice thickness: 1.0 mm; frequency double inversion recovery right/left; minimum repetition time: 60; and auto–repetition time: 600. Tumor sizes were measured and tumor volumes, in cubic millimeters, were calculated by the formula: volume = $(\text{width})^2 \times \text{length}/2$ using Function Analysis software.[7,11] For survival studies, moribund mice or mice with severe neurologic symptoms were euthanized.

Western Blot Analysis

Western blot analysis was performed as previously described.[7,12] The samples of tumor tissues of nude mice in 4 groups were homogenized in a radioimmunoprecipitation assay lysis buffer. Lysates were cleared by centrifugation (14 000 rpm) at 4°C for 30 min. Protein samples (~40 μg) were separated by sodium dodecyl sulfate–polyacrylamide gel electrophoresis (15% gel), transferred to polyvinylidene difluoride membrane and nonspecific binding sites blocked by incubation in 5% nonfat milk for 60 min. Membranes were incubated at 4°C overnight with anti-Rad51 antibody (1:400 dilution; Santa Cruz Biotechnology), anti-c-Met antibody (1:400 dilution; Santa Cruz), anti-SLC22A18 antibody (1:1000 dilution; Santa Cruz), or anti-special AT rich sequence binding protein 1 (SATB1) antibody (1:200 dilution; Sigma). Then the membrane was washed 3 times with Tris-buffered saline and 0.05% Tween 20 for 10 min and probed with the horseradish peroxidase–conjugated secondary antibody (1:2000 dilution; Dako) at room temperature for 30 min. The membrane was developed by an enhanced chemiluminescence system (Pierce) after being washed 3 times.

Statistical Analysis

Statistical analyses and graphs were performed using the Statistical Package for the Social Sciences version 12.0 for Windows. Quantitative values were expressed as mean ± SD. Statistical differences between groups were examined using a Student's *t*-test. $P < .05$ was considered statistically significant.

Results

The Effects of Nano-HAPs on Tumor Cell Radiosensitivity

A decline in clonogenic survival was observed with higher concentrations of nano-HAPs (from 5 to 20 mg/L) for 1 h before 2 Gy irradiation, with a half-maximal inhibitory concentration of 10.7 mg/L in GBM U251 cells and 11.5 mg/L in MDA-MB-231BR cells (Fig. 1A). To evaluate the influences of nano-HAPs on the radiosensitivity of human GBM cells, clonogenic assay was performed on the GBM U251 cells. It was observed that 1 h exposure to 10 mg/L nano-HAPs caused a surviving fraction of ~45% (Fig. 1B), which is in the proper range for determining clonogenic survival in combination with irradiation. For the combination protocol, 1 h after nano-HAPs addition, GBM U251 cells received irradiation followed by a change to nano-HAPs-free medium with colony-forming efficiency, which was evaluated after 12 days. Pretreatment with nano-HAPs increased the radiosensitivity of U251 cells with a dose enhancement factor at a surviving fraction of 0.10 of 1.45, as shown in Fig. 1B. To evaluate whether this radiosensitization was unique to the GBM U251 cell line, our studies were extended to the breast tumor brain metastasis MDA-MB-231BR cell line. Pretreatment for 30 min with nano-HAPs enhanced the radiosensitivity of MDA-MB-231BR cells with a dose enhancement factor at a surviving fraction of 0.10 of 1.40 (Fig. 1B), which resulted in a surviving fraction of 47%.

The Effects of Nano-HAPs on the Apoptotic Phase and Mitotic Index of Tumor Cell

To determine whether the radiosensitization induced by nano-HAPs was the result of accumulation of cells in a more radiosensitive phase of the cell cycle, flow cytometry was used to determine the effects of nano-HAPs on the cell cycle phase distribution of U251 cells. After 1 h of exposure to 10 mg/L nano-HAPs, there was no significant change in the distribution of U251 cells across the cell cycle. Another potential source of radiosensitization was the abrogation of the G_2 checkpoint, which is considered to protect against irradiation-induced cell

death.[13,14] The effects of nano-HAPs on the radiation-induced activation of the G_2 checkpoint were defined according to the method of Xu et al.[15] This experiment investigates the percentage of the mitotic cells in the 4N population according to the specific γH2AX expression in the mitotic cells. Done as a function of time after irradiation, this analysis provided an evaluation of the progression of G_2 cells into M phase and the G_2 checkpoint activation. Irradiation (2 Gy) caused a decrease in the mitotic index by 1 h (Fig. 2A), reaching

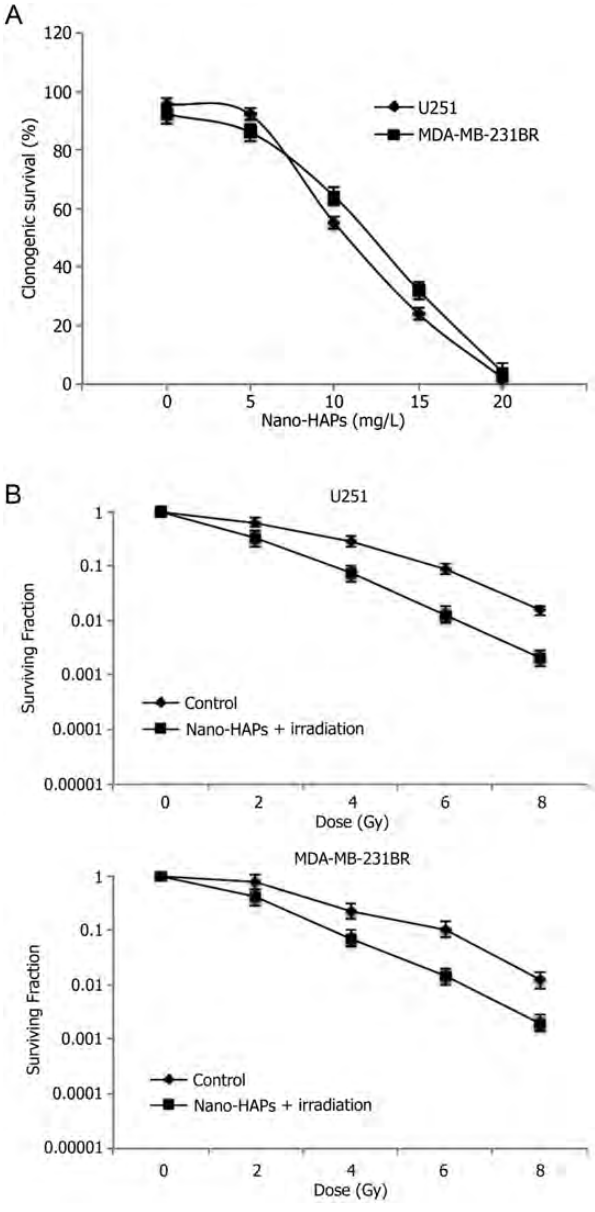

Fig. 1. The influences of nano-HAPs on the radiosensitivity of tumor U251 and MDA-MB-231BR cells. (A) Both U251 cells and MDA-MB-231BR cells were treated with increasing doses of nano-HAPs 5–20 mg/L for 1 h before 2 Gy irradiation. Half-maximal inhibitory concentrations with an incubation time of 1 h before 2 Gy irradiation were 10.7 mg/L in U251 cells and 11.5 mg/L in MDA-MB-231BR cells. (B) Tumor cells were exposed to 10 mg/L nano-HAPs for 1 h before irradiation. Cells were fed fresh growth medium immediately after irradiation. Colony-forming efficiency was determined 12 days later, and survival curves were generated after normalizing for the cytotoxicity induced by nano-HAPs alone.

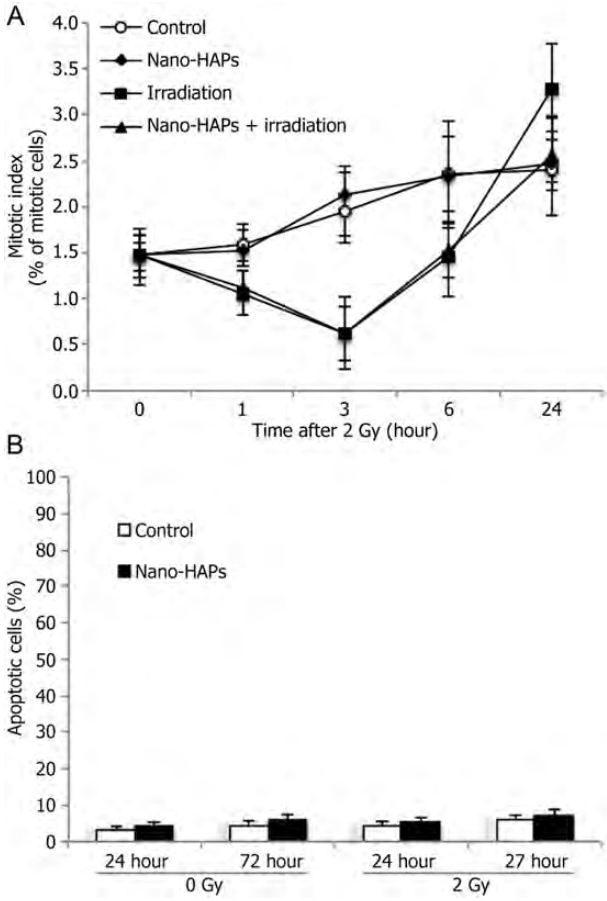

Fig. 2. The effect of nano-HAPs on the mitotic index and apoptotic phase of tumor cells. (A) the effect of nano-HAPs on the mitotic index of tumor cells. U251 cells growing in a 100-mm cell culture dish were stained with propidium iodide at the specified times and analyzed using flow cytometry. To evaluate the activation of the G_2 cell cycle checkpoint, mitotic cells were distinguished from G_2 cells, and the mitotic index was evaluated according to γH2AX expression as detected in the 4N DNA content population by the flow cytometric method. In this assay, a decreased mitotic index reflects the onset of G_2 arrest. Nano-HAPs = cells that had received only nano-HAPs (10 mg/L; 1 h); irradiation = 2 Gy irradiation alone; nano-HAPs + irradiation = nano-HAPs (10 mg/L; 1 h before irradiation) + irradiation. (B) the effect of nano-HAPs on the apoptotic U251 tumor cell phase. Cells grew in a 150-mm cell dish harvested at the specified times. Before analyzed by flow cytometry, 50 μL (3.0×10^4) of treated cell samples were added to a 150-μL staining solution (Guava Nexin assay) containing 135 μL 1 × apoptosis buffer, 10 μL annexin V–phycoerythrin, and 5 μL of 7-aminoactinomycin. Cells were incubated in the dark at room temperature for 20 min. Samples (2000 cells per well) were then acquired on the Guava EasyCyte system. Nano-HAPs = cells that had gained nano-HAPs (10 mg/L; 1 h).

a maximum reduction at 3 h, which indicated that the G_2 checkpoint was activated. Treatment with only nano-HAPs affected neither the mitotic index nor the decrease caused by irradiation. These findings show that radiosensitization induced by nano-HAPs does not involve G_2 checkpoint abrogation. To determine the contribution of apoptosis to the nano-HAPs–mediated radiosensitization of U251 cells, annexin staining was evaluated in U251 cells at 24 and 48 h after irradiation (2 Gy). As expected for solid tumor cells, irradiation resulted in little apoptotic cell death; almost the same level of apoptosis was detected in U251 cell cultures treated with 10 mg/L nano-HAPs only. The combination protocol indicated to enhance irradiation-induced cell death in Fig. 1 did not significantly affect the frequency of apoptotic cell death (Fig. 2B). These results show that nano-HAPs-mediated radiosensitization of U251 cells does not involve enhanced susceptibility to apoptosis.

The Effect of Nano-HAPs on Irradiation-Induced γH2AX Foci

Given that the critical radiation-induced DNA lesion with regard to cell death is the double-strand break (DSB), the influences of nano-HAP exposure on radiation-induced γH2AX foci were analyzed. γH2AX expression has been found to be a sensitive marker of DSBs caused by the clinically relevant doses of ionizing radiation.[16,17] Therefore, to evaluate the influences of nano-HAPs on the induction and repair of DSBs, γH2AX foci were analyzed in U251 cells. U251 cells were exposed to nano-HAPs for 1 h and, as was done in the experiments of cell survival, irradiated (2 Gy), and fed with nano-HAPs-free medium, and γH2AX foci were determined at times as long as 24 h. Cell exposure to only nano-HAPs for 1 h induced a significant increase in the number of γH2AX foci, a level that steadily declined over at least 24 h after removal of nano-HAPs (Fig. 3). Irradiation (2 Gy) resulted in a significant increase in the number of γH2AX foci as detected at 1 h, which further decreased over 24 h. Although the increase above the single treatments was less than additive, exposure to nano-HAPs followed by 2 Gy irradiation induced a larger number of γH2AX foci than either of the single treatments at 1 and 6 h. However, the number of γH2AX foci at 24 h was larger than additive with nano-HAPs + irradiation (24.80 ± 4.16 per cell) compared with the number of γH2AX foci in U251 cells treated with nano-HAPs or irradiation alone (7.62 ± 2.14 and 8.40 ± 3.05 per cell, respectively). The high γH2AX expression in U251 cells 24 h after gaining combined modality suggests a significant inhibition of DNA DSB repair.

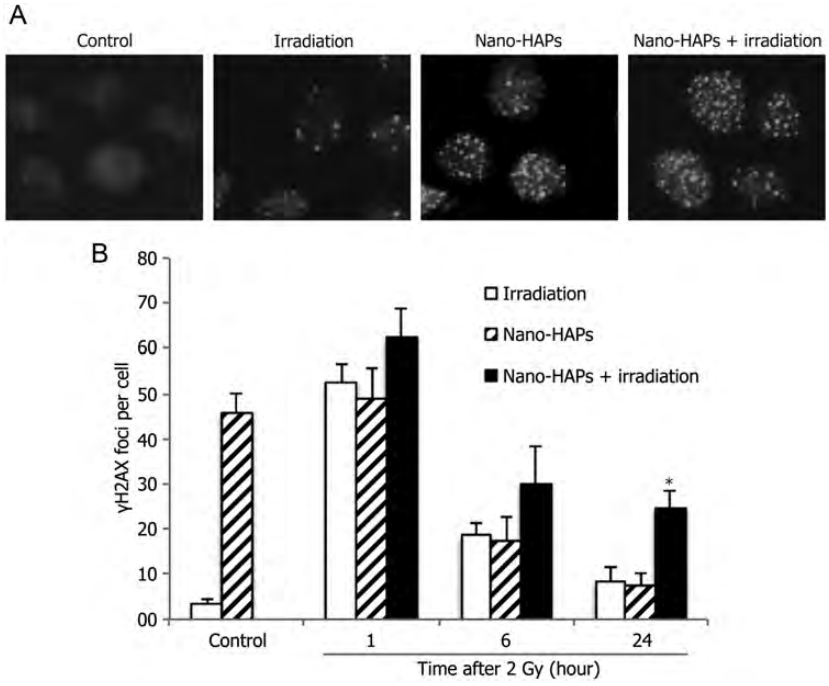

Fig. 3. The effect of nano-HAPs on the γH2AX foci caused by irradiation. U251 cells growing in chamber slides were exposed to 10 mg/L nano-HAPs for 1 h, irradiated (2 Gy), fed fresh medium, and fixed at the specified times for immunocytochemical analysis for nuclear γH2AX foci. Foci were determined in 50 nuclei per treatment per experiment. (A) Representative micrograph images gained from the control cells and cells that had received 10 mg/L nano-HAPs alone for 1 h, 2 Gy irradiation alone, and nano-HAPs (10 mg/L; 1 hr before irradiation) + irradiation at 24 h after irradiation (2 Gy). (B) Vehicle-treated cells (empty columns), cells treated with nano-HAPs alone (hatched columns), and cells treated with the combination of nano-HAPs + irradiation (2 Gy; filled columns). Cells with >5 foci per nucleus were classified as positive for radiation-induced γH2AX. *$P < .01$ according to Student's *t*-test (irradiation vs nano-HAPs + irradiation).

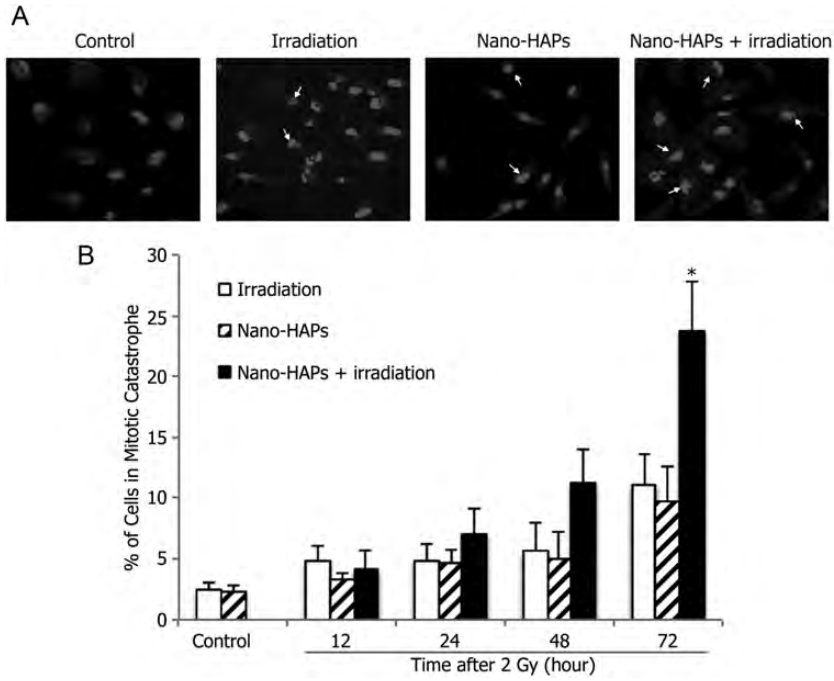

Fig. 4. The effect of nano-HAPs on irradiation-induced mitotic catastrophe of U251 cells. Cells growing in chamber slides were exposed to 10 mg/L nano-HAPs for 1 h, 2 Gy irradiated, fed fresh medium, and fixed at the specified times for immunocytochemical analysis for mitotic catastrophe. Nuclear fragmentation was determined in 300 cells per treatment per experiment. (A) Representative micrograph images gained from control cells and cells that had received 10 mg/L nano-HAPs alone for 1 h, 2 Gy irradiation alone, and nano-HAPs (10 mg/L; 1 h before irradiation) + irradiation at 24 h after 2 Gy irradiation. (B) Vehicle-treated cells (empty columns), cells treated with nano-HAPs alone (hatched columns), and cells treated with the combination of nano-HAPs + irradiation (2 Gy; filled columns). Nuclear fragmentation was defined as the presence of $\geq$2 distinct lobes within a single cell. *$P < .01$according to Student's *t*-test (irradiation vs nano-HAPs + irradiation).

The Effect of Nano-HAPs on Irradiation-Induced Mitotic Catastrophe

The inhibition of DNA DSB repair by nano-HAPs and their failure to enhance irradiation-induced apoptosis of U251 cells suggested that radiosensitization induced by nano-HAPs involves an enhancement in mitotic catastrophe. To verify this hypothesis, mitotic catastrophe was measured according to the cell number, with abnormal nuclei as a function of time after irradiation.[18,19] U251 cells undergoing mitotic catastrophe could be clearly distinguished after individual treatment by irradiation (2 Gy) and nano-HAPs (1 h; 10 mg/L) as well as the combination (Fig. 4A). There was a time-dependent increase in the number of cells undergoing mitotic catastrophe after single treatments with irradiation and nano-HAPs up to at least 72 h after treatment (Fig. 4B). In U251 cells gaining the combination modality, a significantly larger number of U251 cells undergoing mitotic catastrophe were detected at 48 and 72 h posttreatment. These results indicate that nano-HAPs–induced radiosensitization is mediated by an inhibition of DNA DSB repair, leading to an increase in the cells undergoing mitotic catastrophe.

The Effects of Nano-HAPs on Irradiation-Induced Tumor Growth Delay

To determine whether the radiosensitizing effects of nano-HAPs could be extended to an in vivo tumor model, we used tumor cells grown as xenografts in nude mice. The growth rates for U251 and MDA-MB-231BR tumors exposed to each treatment are shown in Fig. 5A. The time to grow from 172 mm^3 to 2000 mm^3 was calculated using the tumor volumes from individual nude mice in each group, and these data were then used to determine the absolute growth delays (the time, in days, for tumors in treated nude mice to grow from 172 mm^3 to 2000 mm^3 minus the time, in days, for tumors to reach the same size in vehicle-treated nude mice). The time required for U251 and MDA-MB-231BR tumors to grow from 172 mm^3 to 2000 mm^3 increased from 18.0 ± 0.5 days and 17.6 ± 0.8 days, respectively, for vehicle-treated nude mice to 28.5 ± 1.8 days and 26.8 ± 2.1 days for nano-HAPs–treated nude mice. For U251 and MDA-MB-231BR tumors, irradiation treatment alone increased the growth time to reach 2000 mm^3 to 30.4 ± 1.5 days and 29.2 ± 1.6 days, respectively.

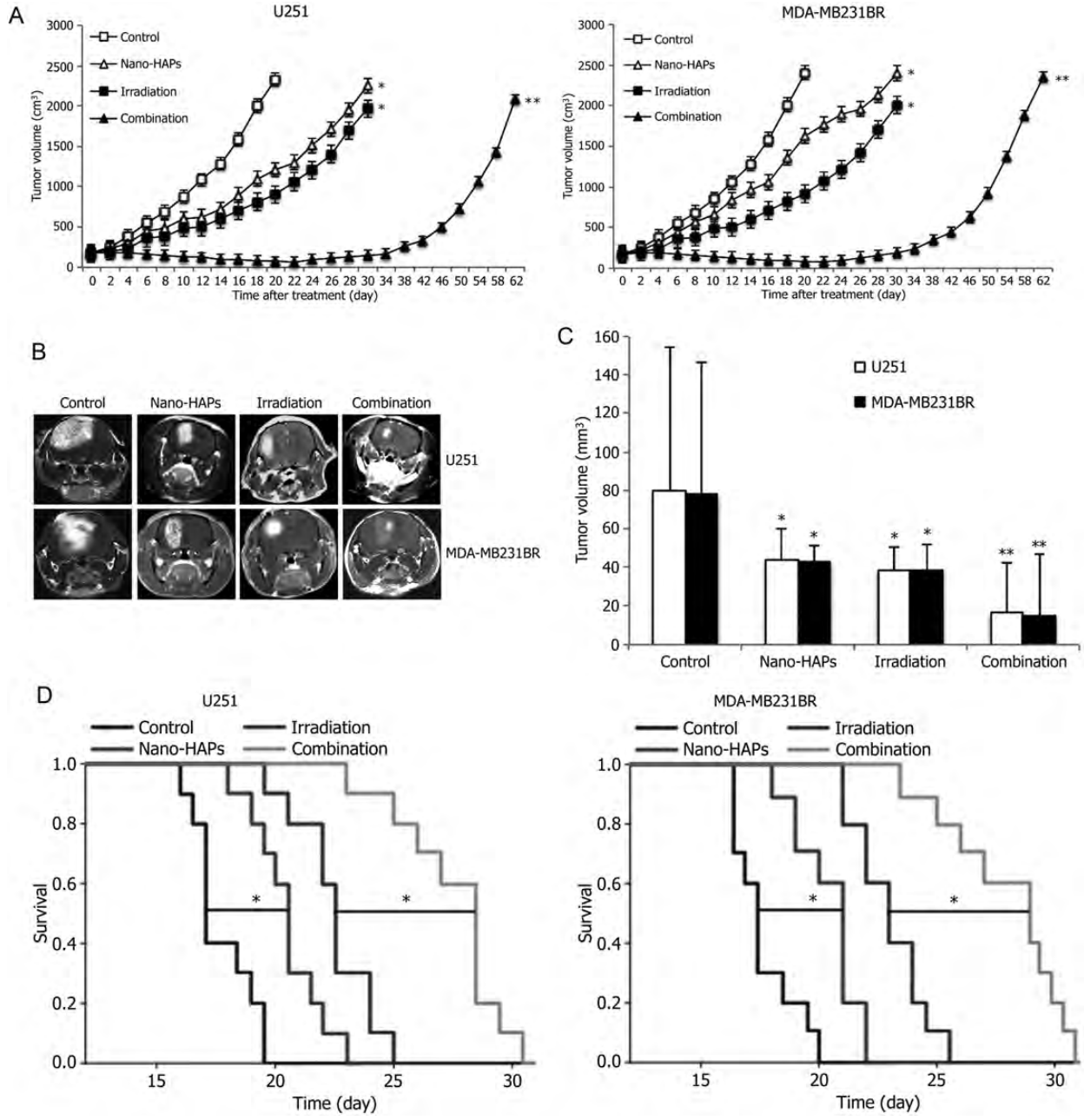

Fig. 5. In vivo antitumor activity of nano-HAPs without or with irradiation in a subcutaneous model and in an independent orthotopic model. (A) Tumor volume in nude mice after being treated with nano-HAPs + irradiation plotted as the mean volume ± SD. When tumors came to 172 mm^3 in size, nude mice were randomized into 4 groups: vehicle, 10 mg/L nano-HAPs, 4 Gy irradiation, and nano-HAPs + irradiation. A single dose of nano-HAPs was delivered by injection through the tail vein at 1 h before 4 Gy irradiation to the tumor. To gain a tumor growth curve, tumor diameters were measured every 2 days with digital calipers, and the tumor volume, in cubic millimeters, was calculated by the formula: volume = $(\text{width})^2 \times \text{length}/2$. Each group contained 10 mice. The findings shown are representative of 2 independent experiments. *$P < .05$ vs control; **$P < .05$ vs control and each monotherapy. (B) The representative images of orthotopic xenograft from the sham-treated control animals and animals that had received nano-HAPs or irradiation or their combination examined by MRI 15 days after tumor injection. (C) Tumor volumes estimated from MRI. *$P < .05$ vs control; **$P < .05$ vs control and each monotherapy. (D) Kaplan–Meier survival analysis of nude mice transplanted intracranially with tumor cells treated with nano-HAPs or irradiation or their combination. Differences between survival curves were compared using a log-rank test. *$P < .05$ for mean survival time.

However, in nude mice that received the combined treatment, the time for U251 and MDA-MB-231BR tumors to reach 2000 mm^3 increased to 61.6 ± 1.2 days and 59.8 ± 1.5 days. The absolute growth delays of U251 and MDA-MB-231BR tumors were 12.4 ± 1.0 and 11.6 ± 0.6 for irradiation alone and 10.5 ± 1.3 and

9.2 ± 1.1 for nano-HAPs alone, and the tumor growth delay of U251 and MDA-MB-231BR tumors caused by the combined treatment was 43.6 ± 0.7 and 42.2 ± 0.7. Thus, the growth delay after treatment by nano-HAPs + irradiation was more than the sum of the growth delays induced by single treatments. The normalized tumor growth delays were calculated to get a dose enhancement factor comparing the tumor radioresponse in nude mice with and without nano-HAP treatment, which accounts for the contribution of nano-HAPs to tumor growth delay caused by the nano-HAPs + irradiation treatment. Normalized tumor growth delay was defined as the time, in days, for tumors to grow from 172 mm^3 to 2000 mm^3 in nude mice exposed to the combined modality minus the time, in days, for tumors to grow from 172 mm^3 to 2000 mm^3 in nude mice treated with nano-HAPs only. The dose enhancement factors, obtained by dividing the normalized tumor growth delay in mice treated with the nano-HAPs + irradiation combination by the absolute growth delay in nude mice treated with irradiation only, were 2.5 and 2.6 for U251 and MDA-MB-231BR tumors, respectively. These results indicate that nano-HAPs significantly enhance the irradiation-induced tumor growth delay of xenografts.

Nano-HAPs Increased Survival in an Orthotopic Model and Enhanced Antitumor Activity of Irradiation

The effect of nano-HAPs without or with irradiation on intracranial (U251 and MDA-MB-231BR) tumor growth was observed by MRI. By day 15, both nano-HAPs and irradiation monotherapies significantly inhibited U251 tumor growth by 44.5% and 51.9%, respectively, vs controls (Fig. 5B and C), which was further reduced by the nano-HAPs + irradiation combination to 79.3%; and both nano-HAPs and irradiation monotherapies significantly inhibited MDA-MB-231BR tumor growth by 45.2% and 50.3% versus controls (Fig. 5B and C), which was further reduced by the combination to 80.8%. The survival curves showed that nano-HAPs alone increased animal survival modestly but statistically significantly compared with controls, with mean survival times of 20.5 and 21 vs 17 and 17.5 days for U251 and MDA-MB-231BR tumors, respectively ($P < .05$, log-rank test; Fig. 5D); for U251 and MDA-MB-231BR tumors, irradiation alone prolonged the mean survival times to 22.5 and 23 days, respectively. For U251 and MDA-MB-231BR tumors, the nano-HAPs + irradiation combination treatment further increased mean survival time to 28.5 and 29 days ($P < .05$ vs respective monotherapies), indicating a supra-additive effect on tumor growth and animal survival between nano-HAPs and irradiation in the orthotopic model.

Nano-HAPs Altered Gene Expression and Pathway Analysis in Tumor Cells in an Orthotopic Model

To further investigate the potential molecular basis of the interaction of nano-HAPs and irradiation, gene expression analysis was conducted on tumor cells in an orthotopic model by Western blotting. As shown in Fig. 6, the Rad51 protein inhibition rate of nano-HAPs monotherapy groups in tumor U251 cells was 63.5% compared with the control group, and the Rad51 protein inhibition rate of the combination treatment group in tumor U251 cells was 66.7% compared with the control group, whereas the Rad51 protein expression in the irradiation monotherapy group significantly increased compared with the control group. There were similar results about c-Met protein expression in tumor U251 cells. Nano-HAPs monotherapy groups and combination treatment groups revealed that the expression of SLC22A18 protein increased, whereas the expression of SATB1 protein decreased in tumor U251 cells. There were similar results about Rad51, c-Met, SLC22A18, and SATB1 protein expression in tumor MDA-MB-231BR cells (Fig. 6).

Discussion

Hydroxyapatite has been widely used as a novel biomaterial for oral cavity medicine and bone damage, is used as a body medicine carrier, and has a good issue compatibility both outside and inside the body.[20–22] Moreover, because nano-HAPs cause very small excitation of blood vessels, feeding medicine could be made by intravenous injection.[23,24] In this study, nano-HAPs were synthesized by the sol-coagel method, which had a good dispersive effect, and the very uniform size of nano-HAPs was ~50 nm, which had the advantage of high surface energy and so on. Our previous study[7] showed that not only did nano-HAPs have an obvious antineoplastic function in glioma cells in vitro and in vivo, but they also reduced the poisonous, adverse reactions to BCNU, strongly cooperated with and decreased the toxicity of certain other chemotherapy drugs, and had a potential for becoming a new clinical antineoplastic drug.

In this study, the results showed that nano-HAPs induced a significant radiosensitization of GBM U251 cells and of breast tumor brain metastatic MDA-MB-231BR cells. The exposure of U251 cells to 10 mg/L nano-HAPs for only 1 h prevented redistribution of cells through the phases of the cell cycle before irradiation and causation of excessive cytotoxicity, allowing for an accurate assessment of the influences of nano-HAPs on radiosensitivity. As the first investigation into the mechanism mediating nano-HAPs–induced radiosensitization of U251 cells, we studied cellular processes known to be determinants of radiosensitivity. These data showed that nano-HAPs exposure did not induce cell redistribution into a radiosensitive phase of the cell cycle, nor did it have an effect on the activation of the G_2 cell cycle checkpoint. Furthermore, the increased susceptibility to apoptotic cell death did not account for the radiosensitization induced by nano-HAPs. As an alternative to apoptosis, irradiation can cause cell death by mitotic catastrophe. In this study, nano-HAPs exposure of U251 cells induced a significant increase in the mitotic catastrophe caused by irradiation, which is consistent with the

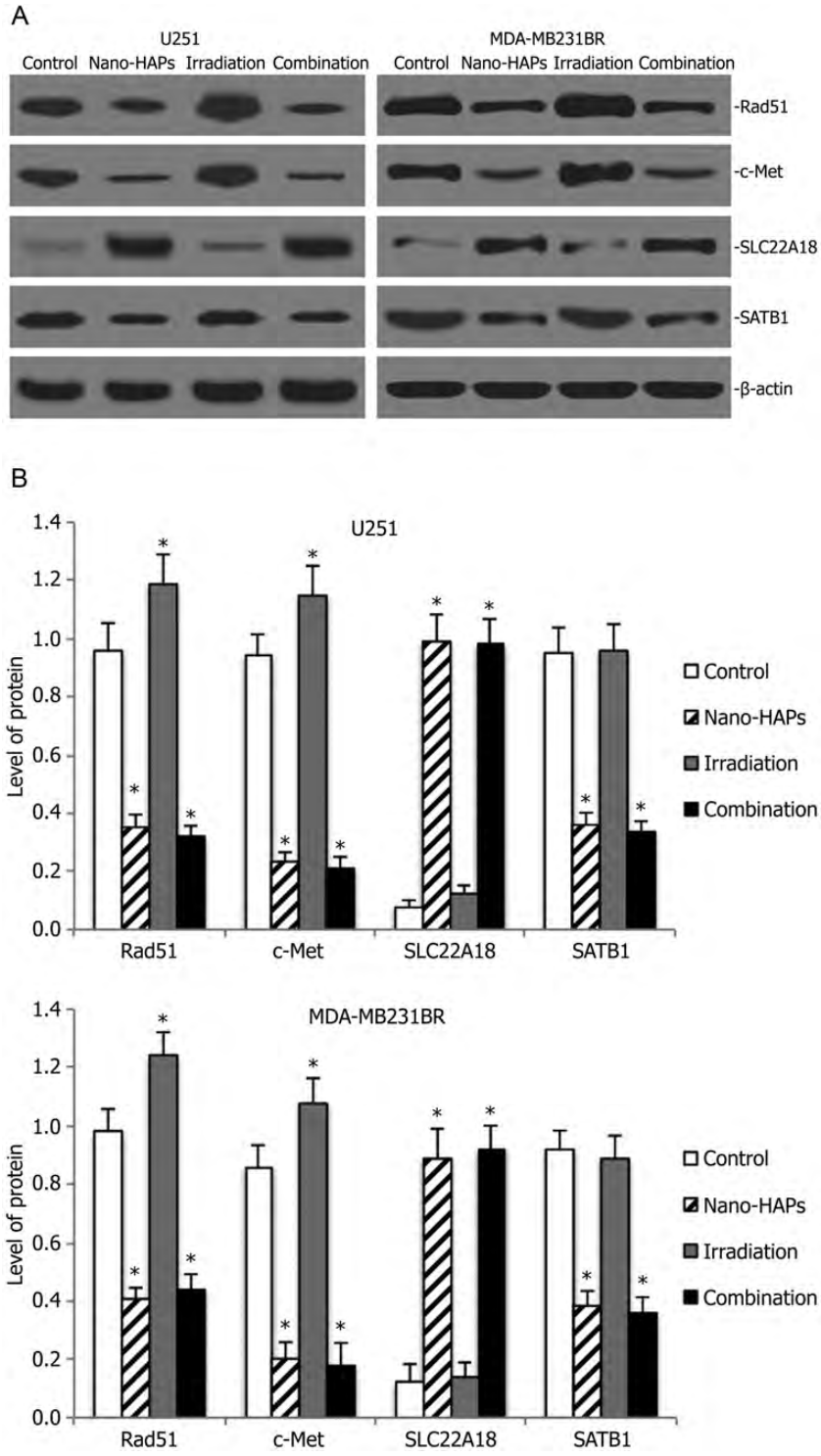

Fig. 6. Western blot analysis for Rad51, c-Met, SLC22A18, and SATB1 expression of orthotopic xenograft from the sham-treated control animals and animals that had received nano-HAPs or irradiation or their combination. (A) Representative images of Western blot analysis. β-actin was used as loading control. (B) Level of Rad51, c-Met, SLC22A18, and SATB1 expression. $*P < .05$ vs control.

putative inhibition of DNA DSB repair, to be described. A very important event in determining radiosensitivity is DNA DSB repair. Recently γH2AX expression has been established as a sensitive marker of DSBs caused by clinically relevant doses of ionizing radiation; and at sites of radiation-induced DNA DSBs, the histone H2AX becomes rapidly phosphorylated (γH2AX), forming readily visible nuclear foci.[16,17] Recent reports show that the dephosphorylation of γH2AX and dispersal of γH2AX foci in irradiated tumor cells correlates

with DNA DSB repair,[25,26] although the specific role of γH2AX in the repair of DNA DSBs has not been defined.[27] Our data showed that γH2AX expression in U251 cells treated with the nano-HAPs + irradiation combination was significantly higher at 24 h after irradiation than that of the monotherapies, which was suggestive of an inhibition of DNA DSB repair. Nevertheless, it is not possible to conclude whether nano-HAPs inhibited the repair of irradiation-induced DSBs or irradiation inhibited the repair of nano-HAPs-induced DNA damage, because nano-HAPs also caused a significant increase in γH2AX that also decreased over the 24-h postirradiation period.

Rad51 is a key player in homologous recombination repair.[28] Rad51 inhibition is an effective means of targeting DNA repair in glioma models, and downregulation of Rad51 can radiosensitize cancer cells.[29] The hepatocyte growth factor/c-Met signaling pathway is upregulated in glioma,[30] with downstream mediators playing a role in DNA DSB repair.[31] Previous studies have shown increased radiosensitization of tumors through modulation of c-Met signaling by genetic methods.[32,33] We have found that SLC22A18 downregulation via promoter methylation and upregulation of SATB1 were associated with the development and progression of glioma,[4,11,34] and elevated expression of SLC22A18 increased the sensitivity of U251 glioma cells to BCNU.[35] Our results showed that nano-HAPs could efficiently downregulate Rad51, c-Met, and SATB1 expression and upregulate SLC22A18 in tumor cells in conferring radiosensitivity. It could also overcome the upregulation of Rad51 and c-Met induced by irradiation.[29,32]

Collectively, our findings show for the first time that nano-HAPs enhanced the radiosensitivity of tumor cells in vitro and furthermore clearly indicate that nano-HAPs could enhance the in vivo radiosensitivity of a GBM xenograft in a subcutaneous model. In an orthotopic model, nano-HAPs increased animal survival alone and increased the irradiation-induced prolongation of the animal life span. Moreover, the radiosensitivity of a cell line corresponding to a breast tumor brain metastasis was also enhanced by nano-HAPs, which suggests that combining nano-HAPs with whole-brain irradiation might be beneficial in brain metastasis therapy. These results show that nano-HAPs could enhance tumor cell radiosensitivity in vitro and in vivo and suggest that this effect involvs an inhibition of DNA repair.

Acknowledgments

The authors thank the East China University of Science and Technology Institute of Biomaterials for providing the hydroxyapatite nanoparticles.

Funding

This work was supported in part by grants from the Innovation Program of Shanghai Municipal Education Commission (12YZ046), the Natural Science Foundation of China (30901535), and the New One Hundred Person Project of Shanghai Jiao Tong University of School of Medicine (10XBR01).

Conflict of interest statement. None declared.

References

1. Ricard D, Idbaih A, Ducray F, Lahutte M, Hoang-Xuan K, Delattre JY. Primary brain tumours in adults. *Lancet*. 2012;379:1984–1996.
2. Chu SH, Ma YB, Feng DF, et al. Correlation of low SLC22A18 expression with poor prognosis in patients with glioma. *J Clin Neurosci*. 2012;19:95–98.
3. Stupp R, Mason WP, van den Bent MJ, et al. Radiotherapy plus concomitant and adjuvant temozolomide for glioblastoma. *N Engl J Med*. 2005;352:987–996.
4. Chu SH, Ma YB, Feng DF, et al. Upregulation of SATB1 is associated with the development and progression of glioma. *J Transl Med*. 2012;10:149.
5. Motskin M, Müller KH, Genoud C, Monteith AG, Skepper JN. The sequestration of hydroxyapatite nanoparticles by human monocyte-macrophages in a compartment that allows free diffusion with the extracellular environment. *Biomaterials*. 2011;32:9470–9482.
6. Yuan Y, Liu C, Qian J, Wang J, Zhang Y. Size-mediated cytotoxicity and apoptosis of hydroxyapatite nanoparticles in human hepatoma HepG2 cells. *Biomaterials*. 2010;31:730–740.
7. Chu SH, Feng DF, Ma YB, Li ZQ. Hydroxyapatite nanoparticles inhibit the growth of human glioma cells in vitro and in vivo. *Int J Nanomedicine*. 2012;7:3659–3666.
8. Russo AL, Kwon HC, Burgan WE, et al. In vitro and in vivo radiosensitization of glioblastoma cells by the poly (ADP-ribose) polymerase inhibitor E7016. *Clin Cancer Res*. 2009;15:607–612.
9. Kil WJ, Cerna D, Burgan WE, et al. In vitro and in vivo radiosensitization induced by the DNA methylating agent temozolomide. *Clin Cancer Res*. 2008;14:931–938.
10. Barker CA, Burgan WE, Carter DJ, et al. In vitro and in vivo radiosensitization induced by the ribonucleotide reductase inhibitor Triapine (3-aminopyridine-2-carboxaldehyde-thiosemicarbazone). *Clin Cancer Res*. 2006;12:2912–2918.
11. Chu SH, Feng DF, Ma YB, et al. Promoter methylation and downregulation of SLC22A18 are associated with the development and progression of human glioma. *J Transl Med*. 2011;9:156.
12. Saratsis AM, Yadavilli S, Magge S, et al. Insights into pediatric diffuse intrinsic pontine glioma through proteomic analysis of cerebrospinal fluid. *Neuro Oncol*. 2012;14:547–560.

13. Bridges KA, Hirai H, Buser CA, et al. MK-1775, a novel Wee1 kinase inhibitor, radiosensitizes p53-defective human tumor cells. *Clin Cancer Res*. 2011;17:5638–5648.
14. Morgan MA, Parsels LA, Zhao L, et al. Mechanism of radiosensitization by the Chk1/2 inhibitor AZD7762 involves abrogation of the G2 checkpoint and inhibition of homologous recombinational DNA repair. *Cancer Res*. 2010;70:4972–4981.
15. Xu B, Kim ST, Lim DS, Kastan MB. Two molecularly distinct G(2)/M checkpoints are induced by ionizing irradiation. *Mol Cell Biol*. 2002;22:1049–1059.
16. de Feraudy S, Revet I, Bezrookove V, Feeney L, Cleaver JE. A minority of foci or pan-nuclear apoptotic staining of gammaH2AX in the S phase after UV damage contain DNA double-strand breaks. *Proc Natl Acad Sci U S A*. 2010;107:6870–6875.
17. Yue J, Wang Q, Lu H, Brenneman M, Fan F, Shen Z. The cytoskeleton protein filamin-A is required for an efficient recombinational DNA double strand break repair. *Cancer Res*. 2009;69:7978–7985.
18. Shang ZF, Huang B, Xu QZ, et al. Inactivation of DNA-dependent protein kinase leads to spindle disruption and mitotic catastrophe with attenuated checkpoint protein 2 phosphorylation in response to DNA damage. *Cancer Res*. 2010;70:3657–3666.
19. Maalouf M, Alphonse G, Colliaux A, et al. Different mechanisms of cell death in radiosensitive and radioresistant p53 mutated head and neck squamous cell carcinoma cell lines exposed to carbon ions and x-rays. *Int J Radiat Oncol Biol Phys*. 2009;74:200–209.
20. Fu Q, Hong Y, Liu X, Fan H, Zhang X. A hierarchically graded bioactive scaffold bonded to titanium substrates for attachment to bone. *Biomaterials*. 2011;32:7333–7346.
21. Singh MK, Gracio J, LeDuc P, et al. Integrated biomimetic carbon nanotube composites for in vivo systems. *Nanoscale*. 2010;2:2855–2863.
22. Fernandez JM, Molinuevo MS, Cortizo MS, Cortizo AM. Development of an osteoconductive PCL-PDIPF-hydroxyapatite composite scaffold for bone tissue engineering. *J Tissue Eng Regen Med*. 2011;5:e126–e135.
23. Hou CJ, Liu JL, Li X, Bi LJ. Insulin promotes bone formation in augmented maxillary sinus in diabetic rabbits. *Int J Oral Maxillofac Surg*. 2012;41:400–407.
24. Sung MS, Kim HG, Woo KI, Kim YD. Ocular ischemia and ischemic oculomotor nerve palsy after vascular embolization of injectable calcium hydroxylapatite filler. *Ophthal Plast Reconstr Surg*. 2010;26:289–291.
25. Neri P, Ren L, Gratton K, et al. Bortezomib-induced "BRCAness" sensitizes multiple myeloma cells to PARP inhibitors. *Blood*. 2011;118:6368–6379.
26. Caron P, Aymard F, Iacovoni JS, et al. Cohesin protects genes against γH2AX induced by DNA double-strand breaks. *PLoS Genet*. 2012;8:e1002460.
27. Malla RR, Gopinath S, Alapati K, Gorantla B, Gondi CS, Rao JS. uPAR and cathepsin B inhibition enhanced radiation-induced apoptosis in glioma-initiating cells. *Neuro Oncol*. 2012;14:745–760.
28. Nakada S, Yonamine RM, Matsuo K. RNF8 regulates assembly of RAD51 at DNA double-strand breaks in the absence of BRCA1 and 53BP1. *Cancer Res*. 2012;72:4974–4983.
29. Short SC, Giampieri S, Worku M, et al. Rad51 inhibition is an effective means of targeting DNA repair in glioma models and CD133 + tumor-derived cells. *Neuro Oncol*. 2011;13:487–499.
30. Chu SH, Feng DF, Zhang H, et al. c-Met–targeted RNA interference inhibits growth and metastasis of glioma U251 cells in vitro. *J Neurooncol*. 2009;93:183–189.
31. Buchanan IM, Scott T, Tandle AT, et al. Radiosensitization of glioma cells by modulation of Met signalling with the hepatocyte growth factor neutralizing antibody, AMG102. *J Cell Mol Med*. 2011;15:1999–2006.
32. De Bacco F, Luraghi P, Medico E, et al. Induction of MET by ionizing radiation and its role in radioresistance and invasive growth of cancer. *J Natl Cancer Inst*. 2011;103:645–661.
33. Chu SH, Zhu ZA, Yuan XH, Li ZQ, Jiang PC. In vitro and in vivo potentiating the cytotoxic effect of radiation on human U251 gliomas by the c-Met antisense oligodeoxynucleotides. *J Neurooncol*. 2006;80:143–149.
34. Chu SH, Ma YB, Feng DF, Zhang H, Qiu JH, Zhu ZA. Effect of 5-Aza-2′-deoxycytidine on SLC22A18 in glioma U251 cells. *Mol Med Report*. 2012;5:138–141.
35. Chu SH, Ma YB, Feng DF, Zhang H, Qiu JH, Zhu ZA. Elevated expression of solute carrier family 22 member 18 increases the sensitivity of U251 glioma cells to BCNU. *Oncol Lett*. 2011;2:1139–1142.